Monodisperse Protein Stabilized Gold Nanoparticles via a Simple Photochemical Process

Abdelghani Housni,[†] Marya Ahmed,[†] Shiyong Liu,[‡] and Ravin Narain*,[†]

Department of Chemistry and Biochemistry, Biomolecular Sciences Program, Laurentian University, 935, Ramsey Lake Road, Sudbury, ON, Canada, and Department of Polymer Science and Engineering, University of Science and Technology of China, Hefei, Anhui, China

Received: April 30, 2008; Revised Manuscript Received: June 9, 2008

Protein stabilized, water soluble gold nanoparticles are essential for biomedicines and biotechnology. Bovine Serum Albumin (BSA) is one of the most abundant proteins. It has a remarkable ability of binding and transporting materials across cell membrane that makes it ideal for drug delivery and very useful for pharmaceutical industry. Herein, we explored the direct synthesis of BSA stabilized gold nanoparticles via a simple photochemical process. BSA stabilized gold nanoparticles are synthesized in one step, using Irgacure (I-2959) as photoinitiator. UV radiation facilitates the easy one step synthesis of protein stabilized gold nanoparticles without any denaturation of the protein, during the process. Polyacrylamide Gel (PAGE) shows that there is no difference in the bands height and mobility of native BSA and UV irradiated BSA. PAGE results are further confirmed by fluorescence spectroscopy of native and UV irradiated BSA. BSA/PEG (polyethylene glycol) mixed monolayer stabilized gold nanoparticles have also been prepared in one step using the photochemical process. Different ratios of PEG to BSA are used to evaluate the particle size and the size distribution of gold nanoparticles. Transmission electron microscope (TEM) and dynamic light scattering (DLS) confirm the presence of nearly monodisperse mixed layer stabilized gold nanoparticles.

Introduction

Colloidal gold nanoparticles are a topic of great interest because of their unique optical and electronic properties.[1–4] Colloidal water soluble gold nanoparticles have an absolute importance in biomedicines,[5–8] biotechnology,[9–11] electronics[12] and catalysis.[13] Controlled synthesis of water soluble gold nanoparticles is important for their use in many applications. Burst and Turkevich methods are two well-known widely used methods for the synthesis of gold nanoparticles.[1–4] One phase Burst method, also called "greener method" can successfully synthesize water soluble gold nanoparticles in one step.[4] All these methods produce the gold nanoparticles of well-defined size ranges. Turkevich method deals with the size range of about 20 nm in diameter.[14] Burst method produces the particles of about 4−5 nm in diameter.[15] Controlled synthesis of gold nanoparticles ranging from 1.5−5.2 nm in diameter has also been reported.[16] A recent study shows that cytotoxicity of gold nanoparticles, is highly dependent on their sizes.[17] For this purpose, another method is required to synthesize the gold nanoparticles of controlled and desirable size. Photochemical method is an appropriate approach for this requirement. Scaiano et al. has reported the synthesis of unprotected water soluble gold nanoparticles in one step, by photochemical method.[18] The size of gold nanoparticles is highly dependent on the intensity of UV light and thus can be controlled. The next step is the synthesis of ligand protected water soluble gold nanoparticles in one step by photochemical method.

Stabilization of gold nanoparticles by the ligand of choice is not only important for their long-term stability but it has also important applications in biomedicines and biotechnology.[5–11] Until now gold nanoparticles have been stabilized by a variety of biomolecules, like proteins, peptides, DNA and carbohydrate moieties.[8,19,21] We have also reported the synthesis of biocompatible water soluble gold nanoparticles, stabilized with glycopolymers and poly(N-(isopropyl)acrylamide) (pNIPAM), by photochemical method.[22] The ease with which nearly monodisperse glyco-functionalized gold nanoparticles were synthesized, provided an encouragement for the controlled synthesis of protein protected gold nanoparticles. Synthesis of protein protected gold nanoparticles is of particular interest to understand the protein's specificity and binding capabilities. One of the most widely used proteins is Bovine Serum Albumin (BSA).[23] Serum albumin is the most abundant protein in blood plasma and it serves as a vehicle for intracellular transportation.[8] Serum albumin is of great importance in pharmacology as the conjugation of drugs to albumin decreases their toxicity.[24] It has also been reported that BSA conjugated nanoparticles show improved stability against flocculation, increased quantum yield and low toxicity. BSA can then be conjugated for the targeting purpose.[25] Typically bioconjugation of nanoparticles is a multistep process. This requires the modification of nanoparticle surface with a linker that can recognize the biomolecule and can also protect the nanoparticle from uncontrolled growth and aggregation.[26,27] Citrate capped, BSA conjugated gold nanoparticles are one example of this process.[26] Herein, we propose the direct synthesis of nearly monodisperse BSA stabilized gold nanoparticles, without the need of a linker to stabilize the gold nanoparticles via a simple photochemical method, as shown in scheme 1.

Another approach is mixed monolayer stabilized gold nanoparticles. Mixed monolayer gold nanoparticles are ideal for drug and gene delivery purposes. Peptide−protein mixed monolayer and peptide-PEG mixed monolayer gold nanoparticles have already been reported.[8,20] PEG is an ideal polymer to effectively create the stealth barrier for hydrophobic gold nanoparticles.[17,20] The cytotoxicity results of PEG stabilized gold nanoparticles

* To whom correspondence should be addressed. E-mail: rnarain@laurentian.ca. Tel: +1705 675 1151 (2186). Fax: +1705 675 4844.
[†] Laurentian University.
[‡] University of Science and Technology.

10.1021/jp803890a CCC: $40.75
Published on Web 07/23/2008

SCHEME 1: Photochemical Synthesis of BSA Stabilized Gold Nanoparticles

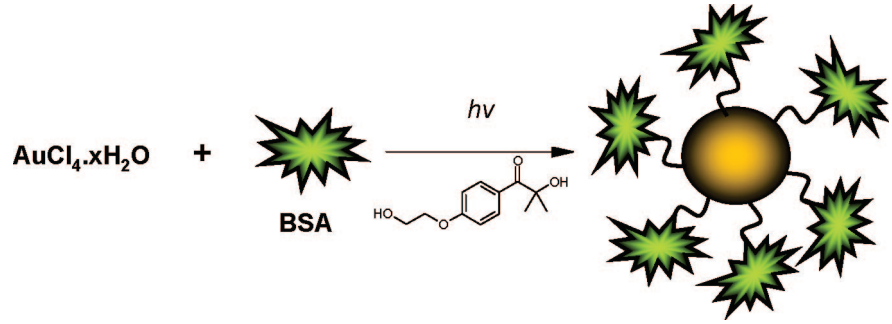

SCHEME 2: Photochemical Synthesis of Mixed Monolayer (BSA/PEG) Stabilized Gold Nanoparticles

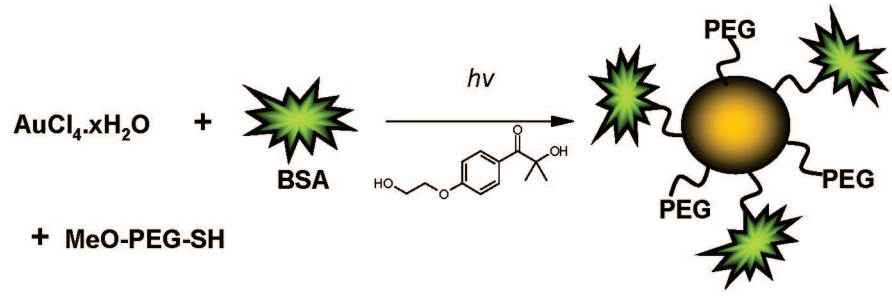

prove the biocompatibility of this molecule. We also propose a one step synthesis of mixed monolayer stabilized gold nanoparticles by the photochemical process, as shown in Scheme 2. PEG/BSA stabilized gold nanoparticles are synthesized by using photochemical initiator Irgacure-2959 in one step. We have also extended this simple photochemical process toward the synthesis of pNIPAM/BSA mixed monolayer coated gold nanoparticles.

Experimental Section

Materials. All chemicals were purchased from Sigma-Aldrich and were used without purification. pNIPAM was synthesized according to reported method[1] and the chain transfer agent, 2-dodecylsulfanylthiocarbonylsulfanyl-2-methyl propionic acid (CTA), was obtained from Noveon Inc.

Methods

Dynamic Light Scattering (DLS). Dynamic light scattering measurements were performed at room temperature using a Viscotek DLS instrument having He−Ne laser at a wavelength of 632 nm and pelltier temperature controller. BSA and pNIPAM stabilized gold nanoparticles solutions and BSA and PEG-SH stabilized gold nanoparticles solutions were filtered through Millipore membranes (0.45 μm pore size). The data was recorded with OmniSize Software.

UV−Visible Spectroscopy. UV−visible absorption spectra (400−800 nm) were recorded on a Cary UV 100 spectrophotometer from the aqueous solutions of BSA and pNIPAM-AuNPs and BSA and PEG-SH-AuNPs at room temperature.

Fluorescence Spectroscopy. Fluorescence measurements were performed on an Olisrsm 1000 (Desa rapid-scanning monochromator spectrophotometry system). The spectra were recorded in the wavelength range of 310−500 nm upon excitation at 295 nm, a 1.00 cm path length rectangular quartz cell was used for this study. Very dilute solutions of native BSA and irradiated BSA concentration of 76 μM were used in the experiment.

Polyacrylamide Gel Electrophoresis (PAGE). PAGE was done on UV irradiated BSA and native BSA, of identical concentrations of 9.1×10^{-5} M.

Typical Synthesis of PNIPAM by RAFT Polymerization. N-Isopropylacrylamide (NIPAM) (2.0 g, 18 mmol, $DP_n = 50$) was dissolved in 5 mL of degassed dioxane. The required amount of RAFT agent CTA (58 mg, 0.2 mmol) and 4,4′-azobis(4-cyanovaleric acid) (12 mg, 43 μmol) were added and the solution was purged with nitrogen. The polymerization was then carried out under nitrogen atmosphere in an oil bath at 65 °C for 24 h. The viscous polymer solution was cooled to room temperature and diluted with deionized water. The polymer solution was dialyzed for 3 days using a dialysis membrane of molecular weight cut off (MWCO) 3400 and the water was changed every 6 h. The polymer was obtained a flaky white solid after freeze-drying overnight.

Photochemical Synthesis of BSA and PEG-SH coated Gold Nanoparticles (BSA and PEG-SH-AuNPs) in the Presence of Irgacure-2959 (IRGC). BSA and PEG-SH coated Au nanoparticles were synthesized by photoirradiation using Irgacure-2959 (IRGC) as a photoinitiator. The molar ratios of $HAuCl_4$, IRGC, BSA and PEG-SH in phosphate buffer were 1:3:0.04:0.06 or 1:3:0.02:0.08. PEG-SH with molecular weight 5 kDa (2.3 or 3.0 mg), 20 kDa (9.2 or 12.2 mg) or 30 kDa (13.7 or 18.3 mg) and BSA (20.4 mg or 10.2 mg, $M_w = 66400$) were used. In a typical synthesis, required amount of BSA and PEG-SH were dissolved in phosphate buffer and solution was added to $HAuCl_4$ (0.80 mg/mL) solution in phosphate buffer. The mixture was stirred using a magnetic stirrer at room temperature for 20 min. Irgacure-2959 (6.09 mM, 1 mL) was dissolved in the mixture of phosphate buffer and MeOH (2:1, v/v). The initiator solution was then added to the $HAuCl_4$ and PEG:BSA mixture and stirred for 20 min. The photoirradiation of the reaction mixture was carried out using sixteen 75 W UV lamps at wavelength a 300 or 253 nm in a Rayonet photoreactor (Southern N.E. Ultraviolet Co.) After 2 h, the reaction mixture was taken off the photoreactor and stirred at room temperature for 20 h. The gold nanoparticles were purified by ultracentrifugation to remove any residual free polymer or free protein.

Photochemical Synthesis of BSA and PNIPAM coated Gold Nanoparticles (BSA and pNIPAM-AuNPs) in the

Presence of Irgacure-2959 (IRGC). The BSA and pNIPAM coated Au nanoparticles were synthesized by photoirradiation using Irgacure-2959 as photoinitiator. The molar ratios of $HAuCl_4$, IRGC, BSA and pNIPAM in phosphate buffer were 1:3:0.04:0.06 or 1:3:0.02:0.08. The pNIPAM with molecular weight ~5 kDa (2.3 or 3.0 mg) and BSA (20.4 mg or 10.2 mg, M_w = 66 400) were used. A similar procedure as described above was carried out for the photochemical synthesis of the BSA and PNIPAM coated gold nanoparticles.

Critical Flocculation Concentration (CFC). The BSA-stabilized Gold nanoparticle were centrifuged at 30,000 rpm for 90 min at room temperature. The modified particles were then resuspended in Phosphate buffer solution. The centrifugation step was repeated three times to ensure complete removal of free BSA. The approximate BSA-stabilized gold nanoparticle concentration of 76 μM was used for Critical Flocculation Concentration (CFC) test. After each 5 min, 10, 100 and 200 μL of 10% NaCl (1.7 M) solution was added to this solution. Then the CFC tests were done by UV−vis measurement in the wavelength range of 400−700 nm.

Results and Discussion

Serum Albumin serves as a depot and transport protein for the endogenous and exogenous compounds. It can bind and transport long chain fatty acids with high affinity and promotes the solubility of fatty acids in plasma. Albumin is also known to bind with billirubin and to decrease its toxicity.[24] These functions of albumin make it suitable for drug delivery process. One of the most studied albumins is Bovine Serum Albumin (BSA). The pronounced capability of BSA to associate noncovalently with small molecules is attributed to the presence of at least six binding domains on the surface of protein. Due to the large number of various ligands that can bind on the surface of protein, the binding capability of protein is regarded as nonspecific.[24] BSA also tends to aggregate with itself in solution, indicating its nonspecific binding. However, BSA is still of great interest in pharmacology due to the biocompatible and water soluble properties, it can render to the drugs. Another factor that makes BSA an interesting vehicle for drug delivery is the presence of numerous functional groups on the surface of BSA that can be further bioconjugated for the targeting purpose.

One way to improve the function of BSA as drug delivery vehicle is by its bioconjugation to gold nanoparticles. Gold nanoparticles themselves have attracted a lot of attention in biomedicine and biotechnology, because of their biocompatibility, optical properties and surface modification capabilities.[1–4] Surface tailoring of gold nanoparticles with BSA can improve the nonspecific binding of BSA.[24] Also BSA conjugated gold nanoparticles can serve as a better drug delivery vehicles compared to BSA alone, as they can be detected in solution due to the optical properties of gold nanoparticles. The surface area of gold can be modified for the targeting purpose and gold nanoparticles render some degree of monodispersity and size control to BSA, which are ideal characteristics for drug delivery. The synthesis of BSA conjugated gold nanoparticles has been a challenge. A number of studies report the synthesis of BSA stabilized nanoparticles, however the synthesis requires multiple steps. The process requires an additional molecule called a 'linker' to stabilize the nanoparticles. The linker also recognizes BSA and immobilizes it on the surface of nanoparticles.[25–30] To the best of our knowledge, Sun et *al.* have reported the direct synthesis of BSA stabilized quantum dots,[23] but there are no reports for the synthesis of BSA stabilized gold nanoparticles, where BSA itself controls the size of gold nanoparticles. BSA is a diverse protein, with many lysine residues on the surface and has only one free thiol at position 34 from the cysteine residue.[19,24] The stabilization of gold nanoparticles by BSA through its thiol group is now documented.[26,35]We therefore assume that the free thiol group on BSA is involved in stabilizing gold nanoparticles.

TABLE 1: Particle Size and Size Distribution of Gold Nanoparticles Synthesized in Sunlight or in a Photoreactor of Wavelength of 300 nm

samples	molar ratio $[AuCl_4]/[I]/[BSA]$	DLS size (nm)	size distr. (DLS)	TEM size (nm)
AuNP-1[a]	1:0.625:0.008	52	0.18	50
AuNP-2	1:0.625:0.008	5	0.71	4
AuNP-3	1:1.25:0.008	8	0.18	5
AuNP-4	1:2.5:0.008	5	0.09	4
AuNP-5	1:3:0.44	4	0.15	4

[a] Experiment done in sunlight.

We have synthesized BSA stabilized gold nanoparticles via a photochemical process in one step, without the requirement of a linker for the stabilization of gold nanoparticles. Photochemistry is a novel approach for the synthesis of gold nanoparticles. Since its introduction by Scaiano et al. only a few manuscripts report the synthesis of nanoparticles by this method..[18,22,31] The method requires a photochemical initiator Irgacure (I-2959) to initiate the reduction of Au^{3+} to Au in the presence of UV light. The intensity of UV light is crucial for the size and shape of nanoparticles.[18,31] As mentioned earlier, the shape, size and narrow size distribution of gold nanoparticles are important factors to consider for their applications. We have therefore focused on the constant intensity of UV light of a wavelength of 300 nm, and used different ratios of initiator to gold salt and gold salt to BSA to determine the optimum conditions for the synthesis of narrow size distribution gold nanoparticles.

The results of some of the experiments conducted using different ratios of initiator to $AuCl_4$ are shown in Table 1. DLS data is also compared to TEM data. The mass distribution from DLS is also compared to the intensity distribution of DLS (Figure-2). Overall we have found that mass distribution by DLS is in close agreement with TEM data. Experiment **AuNP-1** is conducted at room temperature in sunlight, TEM images in Figure 1 (A−C) show that gold nanoparticles obtained are octahedron in shape. TEM also shows that gold nanoparticles are in the size range of 50 nm. The DLS results shown in Table1 are in close agreement with the TEM data. DLS mass distribution confirms the presence of monodisperse nanoparticles of about 52 nm in diameter. The slight difference in TEM data and DLS results is because TEM provides the size of core of nanoparticles, while DLS also takes ligand shell into consideration. The results are in agreement with Scaiano et al. where nearly monodisperse unprotected gold nanoparticles were obtained by sunlight.[18] However in our experiment the particles are BSA protected. It should also be noted that both DLS and TEM data are obtained from samples containing residual free BSA in solution. The results also show that intensity of radiation plays a dominant role in determining the shape of nanoparticles. Wang et al. has successfully synthesized flower shaped nanoparticles by using UV radiation at wavelength of 253 nm.[31] To obtain spherical monodisperse BSA protected gold nanoparticles within minutes, we have focused on UV radiation at a wavelength of 300 nm, and then different initiator to gold ratios are evaluated to obtain monodisperse nanoparticles of controlled sizes. Table 1 shows that while performing the nanoparticles

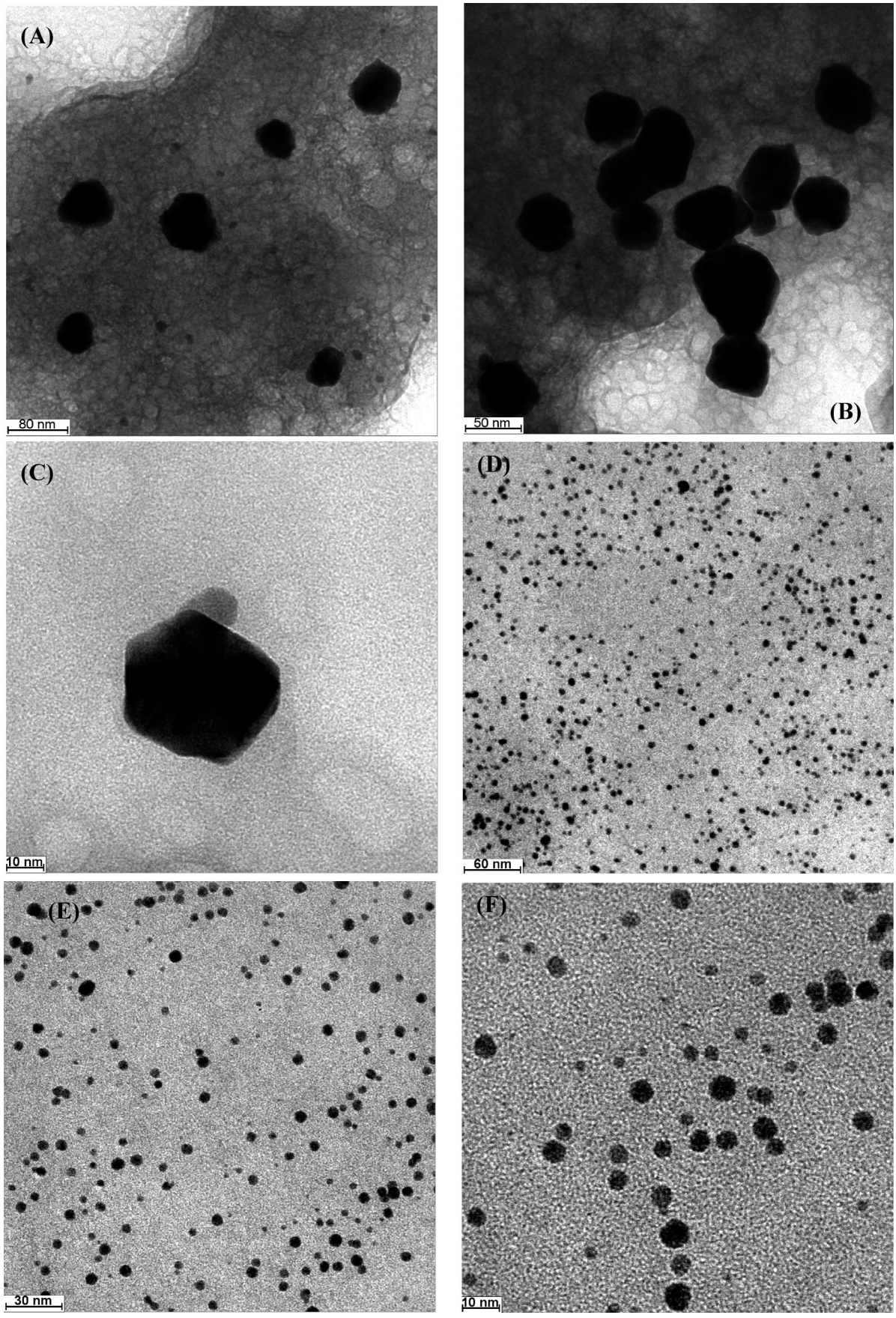

Figure 1. TEM images of BSA stabilized gold nanoparticles generated in sunlight (A−C) (AuNP-1) and in a photoreactor (sample AuNP-2) (D−F) (300 nm) using Irgacure as photoinitiator.

synthesis in a photoreactor, the size and shape of nanoparticles can be controlled. The photoinitiator decomposes quantitatively in the photoreactor which causes a rapid reduction of Au^{3+} to Au^0 and subsequently enhance the nucleation process, thus

TABLE 2: Effect of Polymer Concentration, Molecular Weight of Polymer and Molar Ratio of [$AuCl_4$]/[BSA]/[polymer] on Particle Size and Size Distribution of Nanoparticles.[a]

samples	polymer used	BSA (μM)	polymer (M_n - kg.mol^{-1})	molar ratio [$AuCl_4$]/[BSA]/[polymer]	DLS size (nm)	size distr. (DLS)
AuNP-6	PEG-SH	76.0	5	1:0.04:0.06	12	0.16
AuNP-7	PEG-SH	38.0	5	1:0.02:0.08	8	0.27
AuNP-8	PEG-SH	76.0	20	1:0.04:0.06	13	0.20
AuNP-9	PEG-SH	38.0	20	1:0.02:0.08	9	0.17
AuNP-10	PEG-SH	76.0	30	1:0.04:0.06	13	0.23
AuNP-11	pNIPAM	76.0	~5	1:0.04:0.06	10	0.32
AuNP-12	pNIPAM	38.0	~5	1:0.02:0.08	8	0.29
AuNP-13	−	40.6	−	1:0.02:0	8	0.45
AuNP-14	−	81.3	−	1:0.04:0	6	0.24

[a] Molar ratio of [$AuCl_4$]/[I] is set to 1:3 and gold nanoparticles synthesized in a photoreactor at a wavelength of 300 nm.

providing smaller gold nanoparticles. DLS data show that the nanoparticles have an average diameter of 5 nm with broad size distribution (0.71) when the ratio of $AuCl_4$ to initiator is 1:0.63 (sample AuNPs-2). TEM micrographs of the BSA stabilized gold nanoparticles (Figure 1 (D−F)) show a size range of 4−7 nm in diameter which is in agreement with DLS size distribution. DLS mass distribution is considered more reliable than intensity distribution to measure the hydrodynamic radius of the particles as the mass distribution represents the sizes of the dominating species in solution.[32,33] DLS intensity distribution is useful to determine any aggregation of the nanoparticles in solution. For a better control on the size distribution of the nanoparticles, subsequent experiments were conducted with the increase in molar ratio of initiator to $AuCl_4$. It was found that increasing the molar ratio of initiator to gold salt up to 3 remarkably improves the size distribution of the nanoparticles. TEM images further confirm the presence of relatively monodisperse BSA stabilized gold nanoparticles. Therefore, by setting the ratio of initiator to $AuCl_4$ of 3:1, monodisperse protected gold nanoparticles can be prepared reproducibly. We have also investigated the influence of changing the concentration of BSA on the formation of the nanoparticles and their stability while maintaining the initiator to $AuCl_4$ ratio to 3:1.

The results show that by increasing the concentration of BSA to $AuCl_4$ from 0.02 to 0.04 molar ratio, the size and polydispersity of gold nanoparticles decreases (Table 2). This is in accordance with the results of Wang et al. that report the effect of the concentration of ligand on the size and size distribution of gold nanoparticles.[15] Wang et al. reports the size control of gold nanoparticles using polymeric ligands, the polydispersity obtained by different types of polymers is 0.2 or greater.[15] In this experiment, we have obtained a relatively narrow size distribution of protected gold nanoparticles, using a protein that is known for its aggregation capability. However, over time, we have observed some aggregation of the pure BSA stabilized gold nanoparticles.

To further improve the size distribution and stability of protein stabilized gold nanoparticles for longer period of time, mixed monolayer protected gold nanoparticles were considered. BSA stabilized and mixed monolayer stabilized gold nanoparticles in solution are shown (see Supporting Information S2). The comparison of size and polydispersity of BSA stabilized and BSA and PEG-SH stabilized gold nanoparticles is shown (Figure 2). Therefore, we have first selected polyethylene glycol (MeO-PEG-SH) of varying molecular weights for the synthesis of mixed monolayer gold nanoparticles. Polyethyleneglycol is a biocompatible polymer, which is used extensively to prevent the nonspecific adsorption of serum protein on the drug or gene delivery vehicle.[20] Therefore, one potential advantage of including PEG in mixed monolayer is the prevention of nonspecific adsorption of BSA stabilized gold nanoparticles on surfaces. We have studied the effect of different chain lengths of PEG polymer on the size and polydispersity of gold nanoparticles. Feldheim et al. reports the mixed monolayer stabilized gold nanoparticles, where the mixed monolayer is composed of a peptide and PEG.[8] However, the process of making mixed monolayer stabilized gold nanoparticles requires a multistep reaction pathway and a broad size distribution of the nanoparticles is obtained. The molecular weights of PEG used in this study are 0.9, 1.5 and 5 kDa. It has also been reported that 5 kDa PEG are comparatively better in preventing the nonspecific adsorption of proteins on the nanoparticles. We have therefore used higher molecular weight PEG polymers (5, 20 and 30 kDa) to enhance the stability of nanoparticles and to get a pronounced effect of polymer chain length on gold nanoparticles. We have also studied the effect of varying the molar ratio of BSA to PEG on the stability of the gold nanoparticles. As shown in Table 2, increasing the molecular weight of PEG from 5 to 20 kDa, improves drastically the DLS size distribution of the particles for the PEG to BSA ratio 1:4. (Experiment AuNP-7 and AuNP-9) The slight increase in particle size by DLS is associated with the higher molecular weight of the PEG polymer. However, when the molecular weight of PEG is 30 kDa, there is a slight increase in the size distribution of the nanoparticles. Wang et *al*. has reported the similar results where hydrophobic polymer stabilized gold nanoparticles are compared with PEG stabilized gold nanoparticles.[15] The molecular weight of PEG used in their study is only 3 kDa and the size distribution reported is around 0.2. It has been concluded that hydrophobic polymer chains are better stabilizing ligands for gold nanoparticles as they provide better colloidal stability.[15] The sizes and size distribution of nanoparticles stabilized with the ligand containing BSA to PEG ratio 2:3 are shown in Table 2. It is apparent from the DLS results that the above-mentioned mixed ligand provides some control of the size distribution of the gold nanoparticles. Gold nanoparticles stabilized with the ligand containing BSA to PEG molar ratio 1:4 show that increasing polymer chain length decreases the nanoparticle size distribution. However, with ligand containing BSA to PEG ratio 2:3, the size distribution of nanoparticles increases. (Experiment AuNP-6, AuNP-8 and AuNP-10) This indicates that the stability of the BSA stabilized gold nanoparticles is dependent on dense PEG brushes on the nanoparticles. DLS results indicate that PEG-BSA stabilized gold nanoparticles are much more stable as compared to pure BSA stabilized gold nanoparticles (Figure 2). Furthermore, BSA-PEG stabilized gold nanoparticles do not show aggregation even after 3 weeks.

To further confirm that BSA to PEG ratio 1:4 is better in stabilizing the gold nanoparticles, UV visible spectroscopy is done. UV visible spectrum of nanoparticles with different PEG

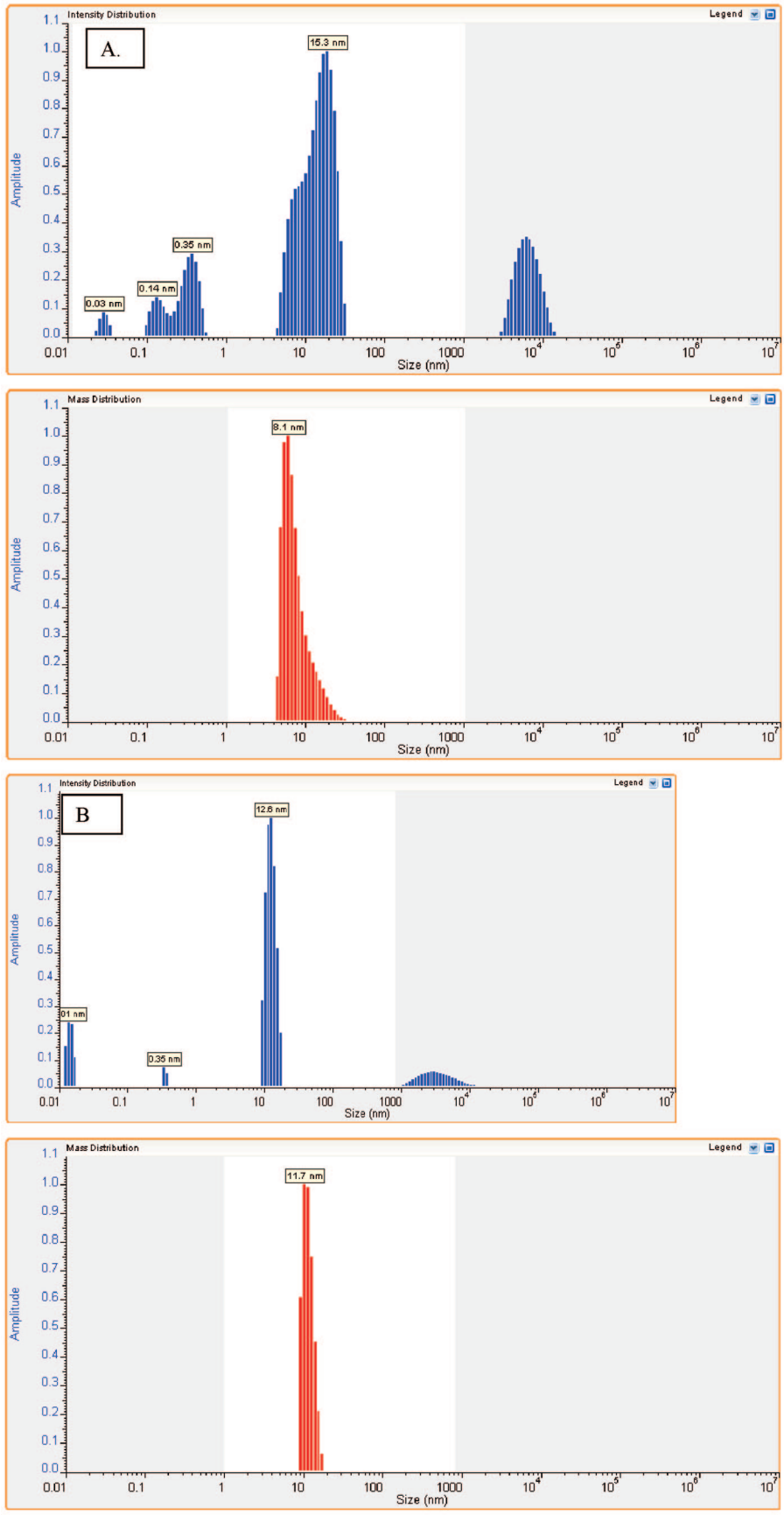

Figure 2. Intensity and mass distribution of BSA stabilized (Experiment AuNP-13) (A) and BSA and PEG-SH stabilized gold nanoparticles (sample AuNP-6) (B).

chain length is shown in Figure 3. The spectrum shows that for BSA to PEG ratio 1:4, regardless of the length of polymer chain, narrow peaks are observed with λ_{max} at 519 nm. This indicated that the gold nanoparticles obtained are small in size and have

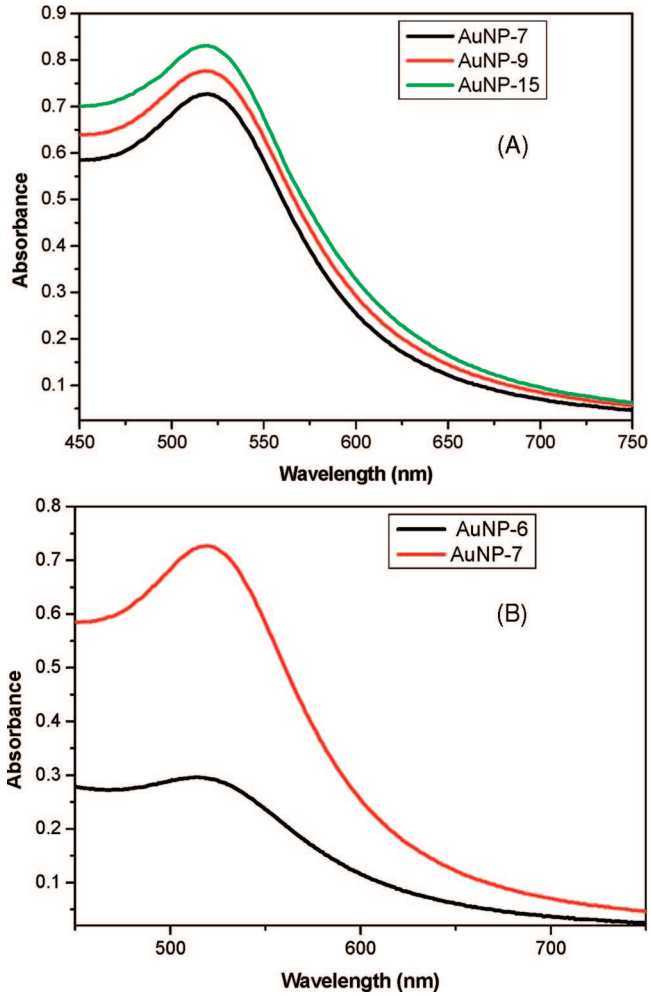

Figure 3. UV−visible spectra of mixed monolayer stabilized gold nanoparticles. The particles are synthesized using BSA and PEG-SH (5, 20 or 30 kDa), by varying the [BSA]/ [PEG] molar ratio: 1:4 (A) and 2:3 (B).

a narrow size distribution. However for the BSA to PEG ratio 2:3, the peaks are broader for all the PEG chain lengths, and λ_{max} is at 514 nm, 509 and 515 nm respectively for 5, 20 and 30 kDa PEG chain length. The broader peaks indicate the formation of aggregates due to larger size or instability of gold nanoparticles. DLS results, as shown in Table 2, confirm that size of nanoparticles having BSA to PEG ratio 2:3 are only slightly larger than the nanoparticles having BSA to PEG ratio 1:4. The broader peaks in UV−visible spectrum of nanoparticles, stabilized with ligand containing BSA to PEG ratio 2:3 are due to the aggregation of nanoparticles. The cause of this aggregation is related to the higher content of BSA in the ligand shell. To prove this, we obtained UV−visible spectra of gold nanoparticles synthesized with increasing concentration of BSA in stabilizing shell, while keeping PEG chain lengths constant. UV visible spectra indicate that the increase in the concentration of BSA in the mixed monolayer causes enormous changes in spectrum (see Figure 4). The increase in concentration of BSA is responsible for the aggregation of nanoparticles and hence the broadening of peaks in UV−visible spectrum. We have also shown that this trend is independent of the polymer chain length used in the stabilizing shell. The increase in the concentration of BSA in mixed monolayer regardless of the PEG chain length in ligand shell, causes aggregation apparent by the broad peak of the spectra (see Supporting Information S3).

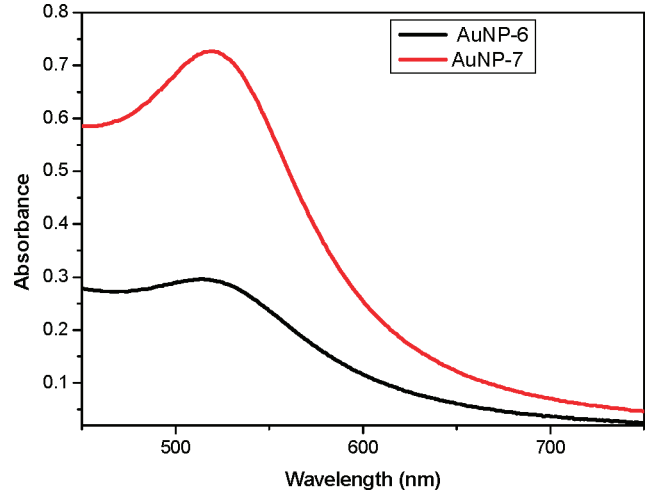

Figure 4. UV−visible spectra of mixed monolayer stabilized gold nanoparticles with increasing concentration of BSA.

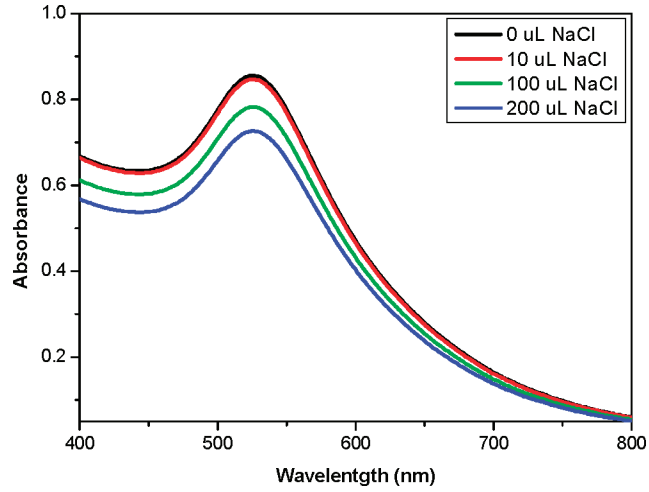

Figure 5. Stability of BSA/AuNPs was assessed by measuring the critical flocculation concentration using 1.7 M NaCl solution. Molar ratio of $[AuCl_4]$/[BSA] were 3:0.02 (AuNP-13).

Once mixed monolayer stabilized gold nanoparticles are obtained, we determined critical coagulation concentration of our samples assess their stability in high salt conditions. It has previously been shown that addition of peptides to gold nanoparticles can decrease their stability in salt solutions.[9,20] Figure 5 shows that with the increase in salt concentration in BSA stabilized gold nanoparticles, there is a slight red shift in UV spectrum, indicating the aggregation. However, it should be noted that even after the addition of 1 M NaCl solution in our sample no visible color change was observed, and λ_{max} shifted only by 1 nm. Thus BSA stabilized nanoparticles are stable to high salt concentration. The stability of mixed monolayer synthesized gold nanoparticles in high salt condition is also studied. The mixed monolayer stabilized gold nanoparticles do not show a red shift in UV visible spectrum even when the salt concentration in solution exceeds to 1 M (see Figure 6 and Supporting Information S4 and S5). This indicates that mixed monolayer stabilized gold nanoparticles are better protected than BSA stabilized gold nanoparticles and are better able to withstand with high salt content.

Another concern while using UV irradiated approach for the synthesis of gold nanoparticles was the denaturation of protein during the process. UV radiation is one of the many factors that can denature the protein, and the physiological functioning

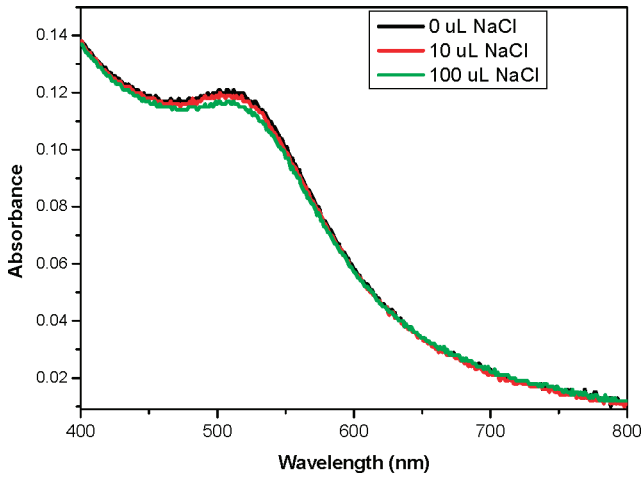

Figure 6. Stability of BSA/PEG-SH AuNPs assessed by measuring the critical flocculation concentration using 1.7 M NaCl solution (sample AuNP-7).

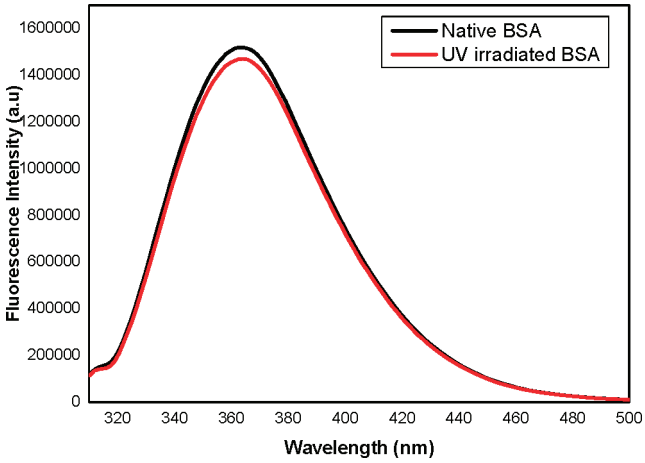

Figure 7. Fluorescence emission spectra of 76 μM BSA before and after UV-Irradiation (300 nm) at pH 7.41 upon excitation at 295 nm in 0.1 M phosphate buffer solution.

of protein is disrupted. To address this issue, we performed polyacrylamide gel electrophoresis (PAGE) on UV irradiated and native BSA (see Supporting Information S6) PAGE results indicate that native BSA and UV irradiated BSA show the exact same pattern. Both of them tend to dimerize and trimerize in buffer solution, indicated by the slow moving bands in the gel. This is a well-known property of BSA that is not denatured.[36] Thus our approach for the gold nanoparticles synthesis by UV radiation does not damage the overall structure of protein. To further confirm our PAGE result, we performed fluorescence spectroscopy on native and UV irradiated BSA samples. Fluorescence spectroscopy is useful to obtain local information about the conformation of protein. BSA has intrinsic fluorescence because of the presence of two tryptophan residue at position 134 and 212. The more specific information about local structure of this protein can be obtained by selectively exciting the tryptophan residues.[19,24] To study this we have performed fluorescence spectrum of native and UV irradiated BSA by exciting the tryptophan residue at 235 nm. As shown in Figure 7, there is almost no change in the emission spectra of native and UV irradiated BSA, indicating that protein is physiologically active.[19,34]

For the purpose of versatility, we have also synthesized pNIPAM/BSA mixed monolayer stabilized gold nanoparticles. Table 2 shows nearly monodisperse particles obtained from the experiments. pNIPAM is a water soluble polymer that exhibits amphiphillic behavior near its lower critical solution temperature (LCST = 32 °C). We have used a one step facile technique for the synthesis of BSA-PEG or BSA-pNIPAM stabilized gold nanoparticles. In future experiments, binding behavior of BSA with different exogenous or endogenous substances in the presence and absence of gold nanoparticles will be studied. The presence of mixed monolayer on the binding behavior of BSA will also be studied.

Conclusion

In conclusion, we have studied the synthesis of BSA stabilized gold nanoparticles by the photochemical process. We have successfully synthesized monolayer and mixed monolayer stabilized gold nanoparticles in one step. We have also studied the effect of concentration of BSA on the core size and polydispersity of gold nanoparticles. DLS data and TEM images have confirmed the presence of relatively monodisperse gold nanoparticles. The polydispersity of mixed monolayer stabilized gold nanoparticles is largely dependent on the concentration of BSA in mixed monolayer. UV visible spectrum obtained for mixed monolayer stabilized gold nanoparticles indicates aggregation with the increase in BSA content. The stability of gold nanoparticles is determined by critical coagulation concentration determination, which indicates the presence of stable nanoparticles in high salt conditions. Finally, PAGE and fluorescence spectrum have confirmed that BSA is not denatured during the photochemical process and it still possess its native conformation.

Acknowledgment. The authors thank Natural Sciences and Engineering Research Council of Canada for financial support of this research work.

Supporting Information Available: TEM micrographs, digital photograph of protected gold nanoparticles, UV−visible spectra of gold nanoparticles and PAGE experiment. This material is available free of charge via the Internet at http://pubs.acs.org.

References and Notes

(1) Dahl, A. J.; Maddux, S. L. B.; Hutchison, E. J. *Chem. Rev.* **2007**, *107*, 2228.
(2) Ghosh, K. S.; Pal, T. *Chem. Rev.* **2007**, *107*, 4797.
(3) Daniel, M-C.; Astruc, D. *Chem. Rev.* **2004**, *104*, 293.
(4) Rosi, L. N.; Mirkin, A. C. *Chem. Rev.* **2005**, *105*, 1547.
(5) Fuente, M. J.; Alcantara, D.; Penades, S. *IEE Trans. Nanobiosci.* **2007**, *6*, 275.
(6) Ojeda, R.; Paz, L. J.; Barrientos, G. A.; Lomas, M.; Penades, S. *Carbohydr. Res.* **2007**, *342*, 448.
(7) Zhou, X.; Zhang, X.; Yu, X.; Zha, X.; Fu, Q.; Liu, B.; Wang, X.; Chen, Y.; Chen, Y.; Shan, Y.; Jin, Y.; Wu, Y.; Liu, J.; Kong, W.; Shen, J. *Biomaterials* **2008**, *29*, 111.
(8) Ryan, A. J.; Overton, W. K.; Speight, E. M.; Oldenburg, N. C.; Loo, L.; Robarge, W.; Franzen, S.; Feldheim, L. D. *Anal. Chem.* **2007**, *79*, 9150.
(9) Medley, C. D.; Smith, J. E.; Tang, Z.; Wu, Y.; Bamrungsap, S.; Tan, W. *Anal. Chem.* **2008**, *80*, 1067.
(10) Schofield, L. C.; Field, A. R.; Russell, A. D. *Anal. Chem.* **2007**, *79*, 1356.
(11) Fuente, M. J.; Penades, S. *Glycoconjugate J.* **2004**, *21*, 149.
(12) Labande, A.; Ruiz, J.; Astruc, D. *J. Am. Chem. Soc.* **2002**, *124*, 1782.
(13) Liu, Z.; Hu, P. *J. Am. Chem. Soc.* **2002**, *124*, 14770.
(14) Li, D.; He, Q.; Cui, Y.; Duan, L.; Li, J. *Biochem. biophys. Res. Commun.* **2007**, *355*, 488.
(15) Wang, Z.; Tan, B.; Hussain, I.; Schaeffer, N.; Wyatt, F. M.; Brust, M.; Cooper, I. A. *Langmuir.* **2007**, *23*, 885.

(16) Hostetler, J. M.; Wingate, E. J.; Zhong, C-J.; Harris, E. J.; Vachet, W. R.; Clark, R. M.; Londono, D. J.; Green, J. S.; Stokes, J. J.; Wignall, D. G.; Glish, L. G.; Porter, D. M.; Evans, D. N.; Murray, W. R. *Langmuir.* **1998**, *14*, 17.

(17) Pan, Y.; Neuss, S.; Leifert, A.; Fischler, M.; Wen, F.; Simon, U.; Schmid, G.; Brandau, W.; Jahnen-Dechent, W. *Small* **2007**, *3*, 1941.

(18) Mcgilvray, L. K.; Decan, R. M.; Wang, D.; Scaiano, C. J. *J. Am. Chem. Soc.* **2006**, *128*, 15980.

(19) Shang, L.; Wang, Y.; Jiang, J.; Dong, S. *Langmuir* **2007**, *23*, 2714.

(20) Liu, Y.; Shipton, K. M.; Ryan, J.; Kaufman, D. E.; Franzen, S.; Feldheim, L. D. *Anal. Chem.* **2007**, *79*, 2221.

(21) Bergen, M. J.; Recum, A. H.; Goodman, T. T.; Massey, P. A.; Pun, H. S. *Macromol. Biosci.* **2006**, *6*, 506.

(22) Narain, R.; Housni, A.; Gody, G.; Boullanger, P.; Charreyre, M.; Delair, T. *Langmuir* **2007**, *23*, 12835.

(23) Meziani, J. M.; Pathak, P.; Harruff, A. B.; Hurezeanu, R.; Sun, Y-P. *Langmuir* **2005**, *21*, 2008.

(24) Hansen, K. U. *Pharmacol. Rev.* **1981**, *33*, 17.

(25) Derfus, M. A.; Chan, C. W.; Bhatia, N. S. *Nano Lett.* **2004**, *4*, 11.

(26) Brewer, H. S; Glomm, R. W.; Johnson, C. M.; Kang, K. M.; Franzen, S. *Langmuir* **2005**, *21*, 9303.

(27) Wangoo, N.; Bhasin, K. K.; Boro, R.; Suri, R. C. *Anal. Chim. Acta* **2008**, *610*, 142.

(28) Raschke, G; Kowarik, S.; Franzl, T.; Sonnichsen, C.; Klar, A. T.; Feldmann, J *Nano Lett.* **2003**, *3*, 935.

(29) Xie, H.; Tkachenko, G. A.; Glomm, R. W.; Ryan, A. J.; Brennaman, K. M.; Papanikolas, M. J.; Franzen, S.; Feldheim, L. D. *Anal. Chem.* **2003**, *75*, 5797.

(30) Wang, L.; Wang, L.; Zhu, C.; Wei, X.; Kan, X. *Anal. Chim. Acta* **2002**, *468*, 35.

(31) Wang, L.; Wei, G.; Guo, C.; Sun, >L.; Sun, Y.; Song, Y.; Yang, T.; Li, Z. *Colloids Surf., A.* **2008**, *312*, 148.

(32) Yang, T.; Li, Z.; Wang, L.; Guo, C.; Sun, Y. *Langmuir* **2007**, *23*, 10533.

(33) Philo, S. J. *AAPS J.* **2006**, *8*, E564.

(34) Royer, A. C. *Chem. Rev.* **2006**, *106*, 1769.

(35) Rangnekar, A.; Sarma, K. T.; Singh, K. A.; Deka, J.; Ramesh, A.; Chattopadhyay, C. *Langmuir* **2007**, *23*, 5700.

(36) Restani, P.; Ballabio, C.; Cattaneo, A.; Isoardi, P.; Terracciano, L.; Fiocchi, A. *Allergy* **2004**, *59*, 21.

JP803890A